

# NUMERICAL STUDY OF THE EFFECTS OF TUNNEL INCLINATION AND VENTILATION ON THE DISPERSION OF HYDROGEN RELEASED FROM A CAR

Koutsourakis, N.<sup>1</sup>, Tolias, I.C.<sup>1</sup>, Giannissi, S.G.<sup>1</sup> and Venetsanos, A.G.<sup>1</sup>

<sup>1</sup> Environmental Research Laboratory, National Centre for Scientific Research "Demokritos",  
P.O. Box 60037, Agia Paraskevi, 15310, Greece, nk@ipta.demokritos.gr,  
tolias@ipta.demokritos.gr, sgiannissi@ipta.demokritos.gr, venets@ipta.demokritos.gr

## ABSTRACT

Hydrogen cars are expected to play an important role in a decarbonised, clean-transport future. Safety issues arise though in tunnels, due to the possibility of accidental release and accumulation of hydrogen. This Computational Fluid Dynamics (CFD) study focuses on the effect of tunnel inclination and ventilation on hydrogen dispersion. A horseshoe shaped tunnel of 200 m length is considered in all seventeen cases examined. In most cases, hydrogen is released from the bottom of a car placed at the center of the tunnel. Various inclinations, in-tunnel wind speeds and fuel tank Pressure Relief Device (PRD) diameters were considered in order to assess their influence on safety. It was found that even if the long-term influence of the inclination is positive, there is no systematic effect at initial stages, nor at the most dangerous 'nearly-stoichiometric' cloud volumes (25% - 35% v/v). Adverse effects may also exist, like the occasionally higher flammable cloud (4% - 75% v/v). Regarding ventilation, it was found that even low wind speeds (e.g. 1 m/s) can reduce the flammable cloud by several times. However, no significant effect on the total nearly-stoichiometric volumes was found for most of the cases examined. Ventilation can also cause adverse effects, as for example at mid-term of the release duration, in some cases. Concerning the PRD diameter, a reduction from 4 mm to 2 mm resulted in about five times smaller maximum of the nearly-stoichiometric cloud volume. In addition, the effect of release orientation on hydrogen cloud was examined and it was found that the downwards direction presents drawbacks compared to the backwards and upwards release directions.

## 1.0 INTRODUCTION

An accidental hydrogen release inside a tunnel can raise certain safety concerns, since flammable cloud can be formed endangering the passengers and pedestrians. The influence of tunnel slope on hydrogen dispersion should be investigated in order to explore the necessity of special safety recommendations. Within the EU-funded project, HyTunnel-CS, the effects of the slope, of the mechanical ventilation, of the PRD diameter size and of the release orientation on hydrogen cloud evolution were examined.

Two different inclinations will be presented and compared with the case of zero inclination as reference case. The main objective is to examine if the tunnel slope assists hydrogen dispersion. Additional objectives of this work are to investigate the effect of release diameter, mechanical ventilation and release orientation on the dispersion of flammable hydrogen cloud. For these purposes, two different nozzle sizes are tested, 2 and 4 mm, three ventilation rates are imposed (along with the no ventilation case as reference) and the downward, backward and upward release directions are examined. For the study, CFD simulations are conducted using the ADREA-HF code, which has been extensively validated against hydrogen dispersion cases [1], [2].

### 1.1 Short review

Most of the tunnels are actually inclined [3]. The reasons for inclination can be physical restrictions, like for example in undersea tunnels, construction or drainage needs and many others. Usually, the slope is a few per cent. According to the current EU Directive 2004/54/EC, new tunnels are not allowed to have a slope higher than 5% (2.86°), unless geographical limitations dictate different approach. An inclined tunnel can have a longitudinal "V", a "Lambda" (inverted "V") or a straight-

line shape. For one-directional circulation, the straight-line tunnel is mentioned as “ascending”, when the vehicles move towards the higher end of the tunnel and “descending” otherwise.

The most significant physical consequence in an inclined tunnel on the dispersion of hydrogen or smoke is the “stack effect”, or “chimney effect” due to buoyancy. The stack effect involves the tendency of lower density gases to be transferred upwards, towards the higher end of the tunnel.

A limited number of studies related to hydrogen dispersion in sloped tunnels can be found in literature. Tunnel inclination has attracted the scientific interest especially concerning its effects on fire and smoke propagation. Smoke and hydrogen are expected to present several similarities due to their buoyant nature and thus several recommendations for smoke might also be applied in hydrogen. Smoke studies at naturally ventilated tunnels with inclination showed that the smoke reaching the ceiling initially expands towards both directions [4]. At later stage though, the ‘stack effect’, increases the propagation speed towards the upper end of the tunnel due to buoyancy [5]. This affects both the flow and the dispersion field [6], especially at long tunnels and high inclinations [7]. At mechanically ventilated tunnels, the critical velocity, in order to avoid back-layering, slightly increases as the slope increases [8]. However, several times higher pressure increase should be delivered from the ventilation system to achieve the required critical speed at descending tunnels, due to the flow resistance that the stack effect imposes [9]. The case of descending tunnels is one of the most unfavorable concerning safety [10] and should be carefully examined for several positions of the source, especially due to the fact that occasionally confusion may be created about how to act in emergency [3].

The work of Mukai et al. [11] deserves special attention, since it examines hydrogen dispersion in inclined tunnels. Three cases were examined: 1) “Lambda” type (inverted “V” in the longitudinal direction) horseshoe-shaped tunnel with dimensions of  $10 \times 7 \times 50 \text{ m}^3$  (W x H x L) and an inclination of 2%, 2) V-type rectangular tunnel with dimensions of  $10 \times 4.5 \times 50 \text{ m}^3$  and an inclination of 5%, and 3) “Lambda” type horseshoe-shaped tunnel with dimensions of  $10 \times 7 \times 200 \text{ m}^3$  and an inclination of 2%. In all cases the tunnels were uni-directional with 2 lanes, without ventilation. Five cars were considered and modeled as boxes with dimensions of  $4.7 \times 1.8 \times 1.7 \text{ m}^3$ . The leakage was horizontal, from the rear of the front-most car, which was supposed to stop mid-way. The leak rate was only 133 L/min (20°C), for a period of 30 minutes and the leak hole was square with sides of 0.05 m. The STAR-CD CFD code was employed, with the  $k-\varepsilon$  turbulence model. The results revealed that in all cases the potential risk due to a hydrogen-air mixture above the lower flammability limit is negligible, since only the core of the upward jet close to the car had volume concentrations above 4%.

Seike et al. [12], examine the thermal fume behavior of a hydrogen fuel cell vehicle on fire in a non-ventilated tunnel. The CFD simulations do not include hydrogen dispersion but are mentioned here since three different tunnel inclinations are studied (0%, 2% and 4%). As expected, as the slope increases, at the downwind side the fume propagates faster, while at the upwind side the fume propagation distance decreases. For example, at 240 s after the ignition, the thermal fume has arrived at an upwind distance (from the fire point) of about 129 m for 0%, of about 99m for 2% and of about 67m for 4% inclination, respectively.

## **2.0 EXAMINED SCENARIOS**

In the next Sections the examined scenarios are described along with the numerical setup for each scenario. In all simulations the ADREA-HF CFD code was used.

### **2.1 No ventilation cases**

A realistic hydrogen release scenario from a hydrogen car was considered in order to study the effect of tunnel inclination on hydrogen dispersion. 6 kg of hydrogen were released vertically down below a car from the Pressure Relief Device (PRD) of a 700-bar compressed-hydrogen tank. The blowdown from the high-pressure hydrogen car was considered. Two PRD diameters were studied, one of 4 mm and one of 2 mm.

Figure 1 presents the geometry of the examined problem. A typical horseshoe-shaped tunnel was selected with a length of 200 m, a maximum height of 7.1 m and a width (at the road level) of 9.2 m. Two simple car models with dimensions  $4.2 \times 1.8 \times 1.3 \text{ m}^3$  were placed at the centerline of the tunnel. Hydrogen was released from the bottom of the first car. The source was located at the center of the tunnel and at a distance of 0.5 m from the back of the car and 0.2 m from the ground. Stagnant atmospheric conditions were assumed (no ventilation).

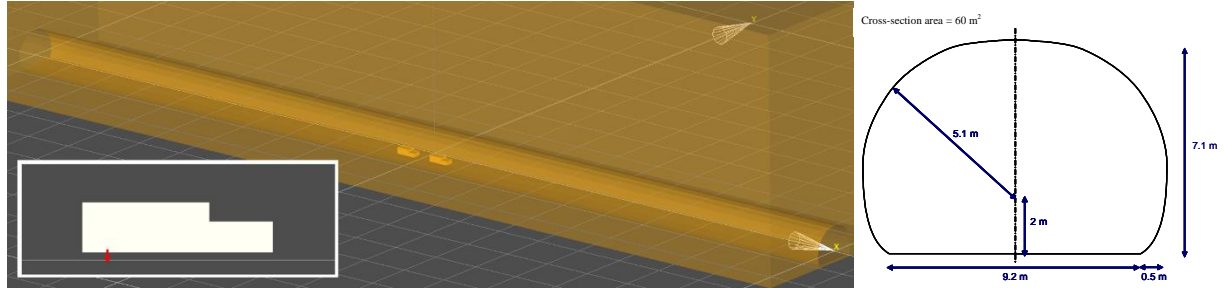


Figure 1. Tunnel geometry (left), cross section (right) and car geometry indicating the release position and direction (inset)

Three tunnels will be presented, with slopes equal to 0%, 2.5% and 5% (descending). Descending tunnels are considered as the worst case, since buoyancy pushes hydrogen towards the area where the trapped people are. Moreover, in case of ventilation, confusion might be created about how to react.

### 2.1.1 Numerical set-up

A notional nozzle approach was used, as Best Practice Guidelines suggest [13], in order to avoid the simulation of the complex shock structure near the release point due to the under-expanded jet that is formed. The Birch approach [14] combined with the NIST equation of state was followed. A constant sonic velocity (equal to about 1305 m/s) and a variable notional nozzle area were considered in order to account for the blowdown. The release duration is approximately 100 s and 400 s for the 4 mm and 2 mm cases, respectively. The computational grid is extended outside the tunnel in all directions in order to minimize the effect of boundary conditions. The dimensions of the domain are  $260 \times 40 \times 42 \text{ m}^3$ . Figure 2 displays some views of the computational grid.

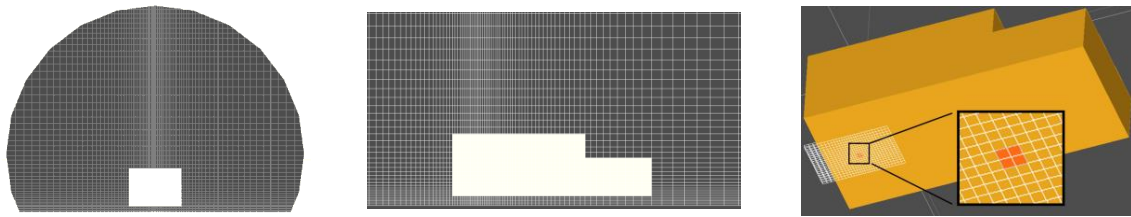


Figure 2. Computational grid for the 4 mm case. Details of the grid around the release (red) area are shown in the right figure

Four cells were used to discretize the release area, at both the 2 mm and the 4 mm cases. Based on preliminary tests and given the unsteady nature of the problem and the simulation uncertainties, the grid resolution of four cells for the source was considered as a good compromise between accuracy and simulation time. The grid around the release is uniform and then increases with an expansion factor of 1.04 - 1.1. In the 2 mm case, symmetry was assumed in the simulations and half of the tunnel is solved. The total number of active cells is equal to 1.1 million for the 4 mm case and 1 million (for half of the tunnel) for the 2 mm case. Two grid sensitivity tests were performed. The first one for the 4 mm case, with a grid resolution of one cell at the source (instead of four) and total number of active cells about 0.2 million for the whole tunnel and the second one for the 2 mm case, with 16 cells (instead of four) discretization of the source and total number of active cells about 1.9 million for half

of the tunnel. The results showed that the general flow characteristics are the same, regardless of the grid density. There is a tendency though for generally higher concentrations at the ceiling, for denser grids. Quantitatively, the coarse grid of the 4 mm case results in about 7% lower maximum volume of the flammable cloud and the fine grid of the 2 mm case results in about 8% higher maximum of flammable cloud. In both cases, the 25% - 35% v/v cloud volume maximums, which are the most important concerning the safety, are practically the same with those of the standard grids.

The  $k$ - $\varepsilon$  turbulence model is used in this study with small initial values of  $k$  ( $0.0025 \text{ m}^2/\text{s}^2$ ) and  $\varepsilon$  (about  $4 \cdot 10^{-4} \text{ m}^2/\text{s}^3$  near walls and  $1 \cdot 10^{-5} \text{ m}^2/\text{s}^3$  at the centerline). Tunnel slope was modelled by changing the gravitational direction in the momentum equations and by setting the appropriate initial hydrostatic pressure. The MUSCL numerical scheme, which exhibits very good results in impinging jets simulations [15], was chosen for the discretization of the convective terms of all equations.

## 2.2 Ventilated cases

A non-ventilated tunnel is a good starting point in order to examine the tunnel slope effects on hydrogen dispersion. It can also be used as a reference case. In reality though, all tunnels are expected to have at least a small ventilation. Even in the cases where there is no mechanical ventilation, the pressure differences between the edges of the tunnel, or the moving vehicles for example (that can cause the “piston effect”), may be enough to establish a small air flow inside the tunnel. Thus, it was considered necessary to additionally examine moderately ventilated tunnels for various inclinations.

For the ventilated scenarios only the PRD of 2 mm was used, since from the results of the no-ventilation cases it was clear that the 2 mm PRD should be preferred against the 4 mm PRD, for safety reasons (see Section Results and discussion). Bulk in-tunnel ventilation velocities of 0.5 m/s, 1 m/s and 2 m/s for slopes of 0%, 2.5% and 5% were examined. A simulation where the ventilation stops five seconds after the start of the release was also performed, in order to study the case in which the ventilation is caused from the piston effect and the cars stop moving due to an accident. This can also happen if the mechanical ventilation fails, due to a fire, for example. Descending tunnels were studied since they were expected to represent the most unfavorable scenario, due to the fact that the stack effect in that case acts against the ventilation and this might trap hydrogen inside the tunnel, especially if the ventilation stops.

### 2.2.1 Numerical set-up

The tunnel geometry, the positions of the cars, the release position and duration and most simulation parameters in general, were the same as in the non-ventilation cases with the PRD of 2 mm. The main difference was the computational domain, which was restricted to the tunnel itself, with no extension outside. This way the flow is more easily controlled and the bulk velocity can be defined with accuracy. An additional advantage is that the number of cells and thus the calculation time are smaller. This is a common configuration for ventilated tunnels in the literature (see for example [16]-[19]).

At the inlet, a uniform velocity parallel to the ground is considered, while at the other end of the tunnel, pressure outlet is applied. All cases tested were initialized from converged, ventilation-only runs, with no hydrogen. Such runs were performed for both with and without domain extensions and in-tunnel flow results did not differ. Symmetry is considered and the number of active cells of half-tunnel is about 800,000. The maximum CFL number in whole domain was assured to be less than 8. In general, the results are presented as comparisons between the various cases/ inclinations and thus any modelling inaccuracies are generally not expected to affect the conclusions.

## 3.0 RESULTS AND DISCUSSION

First, a comparison for the non-ventilated cases is presented. Figure 3 shows the hydrogen iso-surfaces of 10% for the case without slope for 4 mm and 2 mm release diameter at 2 s and 5 s. In 4 mm case, hydrogen jet impinges to the road surface with a speed of some hundreds m/s and spreads over the

street reaching the tunnel walls. Four ‘tongues’ are created, two at the corner of the back of the car and two at the middle of it, which transfer most of the hydrogen upwards. In the 2 mm case (Figure 3, bottom), hydrogen spreads less (horizontally) due to lower flow rate. As a result, it elevates quickly surrounding the car.

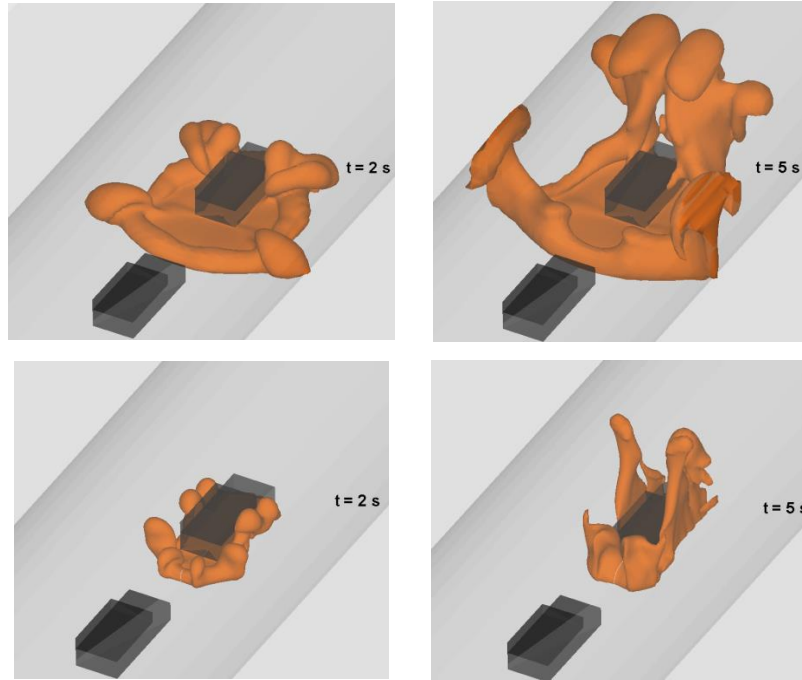


Figure 3. Hydrogen volume concentration iso-surface of 10% for 4 mm (top) and 2 mm (bottom) release diameter at 2 s and 5 s after start of the release for the no slope case

As hydrogen accumulates and rises towards the top of the tunnel, an impinging-like flow is formed at the ceiling for both 2 mm and 4 mm cases. This is shown in Figure 4 where the hydrogen iso-surfaces of 10% vol. and the velocity contours for the 2 mm (top figures) and 4 mm (middle figures) release diameters are presented at 20 s for 0% slope case. We observe that high velocities of about 2 and 3 m/s are developed above the car for the 2 mm and 4 mm case, respectively. The impinging-like jet hits the ceiling and spreads along the tunnel in both directions, again with high velocities. The velocities in the 2 mm case are lower due to the lower mass flow rate at the release during the first 20 s.

In Figure 4 (bottom), the hydrogen iso-surfaces (of 10% vol.) and velocity contours are presented for the 4 mm and 5% slope case. We observe that the impinging-like flow is also formed in the sloped case. Both hydrogen iso-surfaces and the velocity field are similar to the 0% case (Figure 4 - middle). The only noticeable difference in hydrogen iso-surface is that it is inclined towards the entrance of the tunnel due to buoyancy. In the velocity field, the main difference is that the impinging jet has been moved to the back of the car.

In Figure 5, the propagation of hydrogen with time for the 4 mm case is shown for the 0% and the 5% slope case, respectively. Red area is the area above the Lower Flammability Limit of 4% vol. and the yellow area corresponds to the range of 1% till 4% volume concentrations. We observe that hydrogen spreads in both directions of the tunnel in both slope cases. In 0% case, a gap is formed upon the release area due to the impingement-like flow and to the decrease of the flow rate. On the other hand, in 5% case and mainly at the right, this gap does not exist because of buoyant effects. When it comes to flammable cloud spread length, we observe that in 0% case hydrogen reaches the exit of the tunnel and escapes through it, whereas in the case of 5% slope, hydrogen cannot reach the right (low) exit due to buoyancy, so it is trapped inside the tunnel and it is pushed back towards the release area and then towards the upper end of the tunnel. Similar remarks are drawn for the 2 mm case.

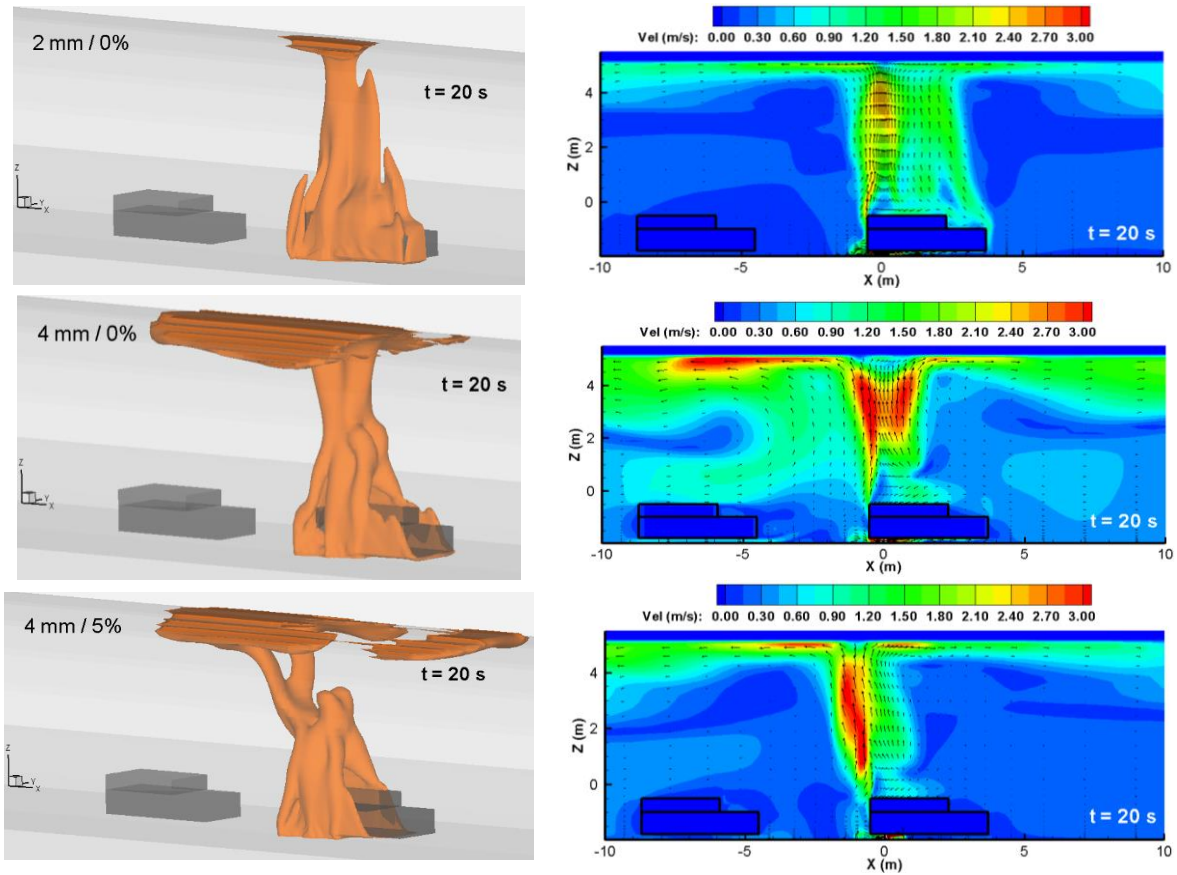


Figure 4. Hydrogen volume concentration iso-surface of 10% vol. and velocity contours for 2 mm/0% slope (top), 4 mm/0% slope (middle) and 4 mm/5% slope (bottom) at 20 s

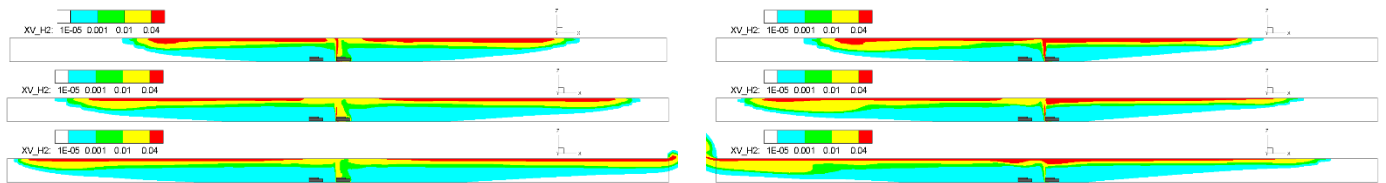


Figure 5. Hydrogen volume concentration contours for 0% slope (left) and 5% slope (right) for the 4 mm case at 60 s, 80 s and 100 s

In Figure 6, the battle between the impinging jet flow at the ceiling and the flammable cloud that is pushed towards the entrance of the tunnel due to buoyancy (5% slope) is presented for the 2 mm case at 260 s. We see that the generated flow field forms a ‘curtain’ that hinders hydrogen move to the left (air curtain effect). That effect is not noticed at the 4 mm case, because the release has stopped before the main mass of hydrogen of the lower end of the tunnel has started moving towards the upper end.

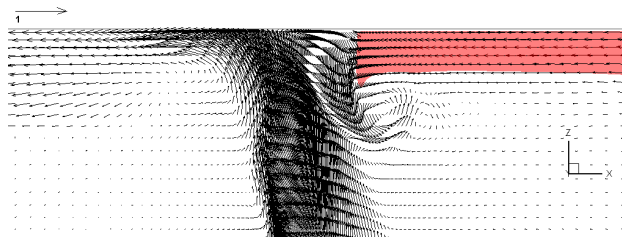


Figure 6. Flow field and hydrogen contour of 4% vol. at 260 s for the 2 mm/5% slope case



In Figure 7 the flammable clouds (4% - 75% volume concentration) and hydrogen cloud volumes of 10% - 75% vol. are presented as functions of time for both release diameters and for all slope cases. Regarding the flammable cloud for the 4 mm case, we see that differences exist among the different slopes only after the end of the release. We observe that at times greater than 150 s, the 2.5% slope has higher values than the 0% case. However, flammable cloud vanishes earlier as slope increases, which is positive in terms of safety. In the 2 mm case, the flammable cloud for the sloped tunnels achieves higher maximums compared to the zero-slope case. The lingering trapping of hydrogen at the right part of the tunnel plays a critical role on this. Comparing the clouds between 4 mm and 2 mm cases, we observe that the reduction of flammable cloud in 2 mm case is less than expected (given the fact that the release area is 4 times smaller), especially for the sloped cases.

Hydrogen clouds of 10% - 75% vol. are more significant in terms of the overpressure that will be produced in case of an ignition. We observe that the specific cloud volume is significantly lower than the flammable volume. Moreover, contrary to the flammable volume, the effect of slope is minor in both 4 and 2 mm cases. Comparing the clouds between 4 and 2 mm cases, we observe that the decrease of the maximum volume in the 2 mm case is significant - approximately 4 times lower maximum volumes. However, we should note that due to the longer release duration of the 2 mm case (400 s against 100 s of the 4 mm case), the 2 mm case exhibits higher cloud volumes compared to the 4 mm case after approximately 25 s.

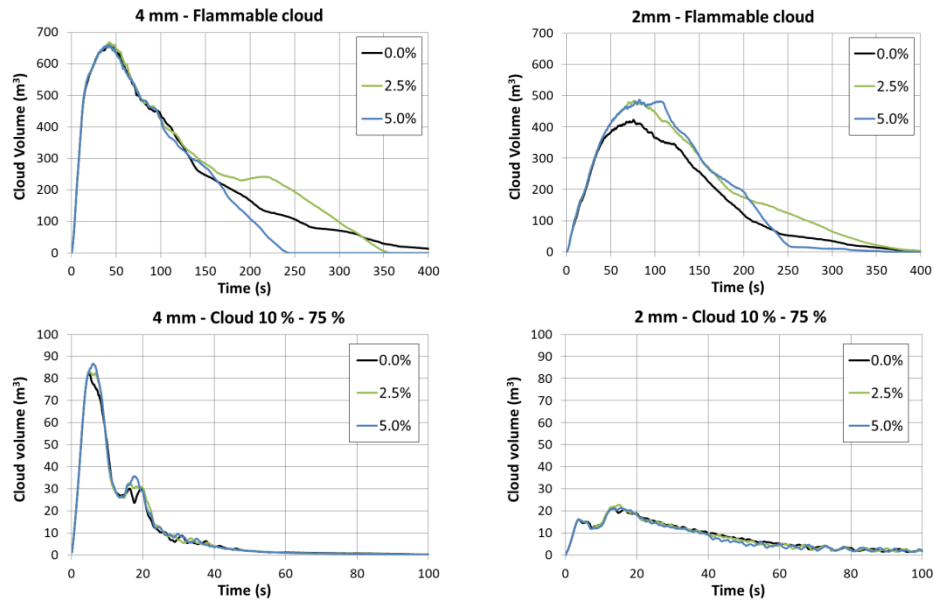


Figure 7. Evolution of hydrogen cloud volumes of different concentration ranges (4% - 75% vol. and 10% - 75% vol.) for various slopes and PRD diameters of 4 mm (left) and 2 mm (right)

At the area above the cars, it was observed that near the end of the release, concentration suddenly increased in all examined cases. The reason is the end of the impinging-like flow at the ceiling when emission stops, which allows hydrogen to fill the ‘gap’ due to diffusion from the neighbor regions.

In the next paragraphs of Section ‘Results and discussion’ the ventilated cases are presented. To get a general overview of the effects of inclination and ventilation, the mid-tunnel concentration contours are shown for various times (Figure 8). It is obvious that the concentration field is completely different in case of ventilation. In general the average concentrations are lower and the flammable part is almost absent at the symmetry plane of the tunnel, even with a small ventilation of 1 m/s. On the other hand, after the time of 60 s, the cloud spreads across the whole tunnel height downwind. The effect of slope is minor at the 1 m/s case and results in a small tendency for backlayering at the ceiling of the tunnel. It should be noted though that at ventilation cases, hydrogen spreads mainly from the sides of the car - it does not surround the whole car as in no-ventilation cases.

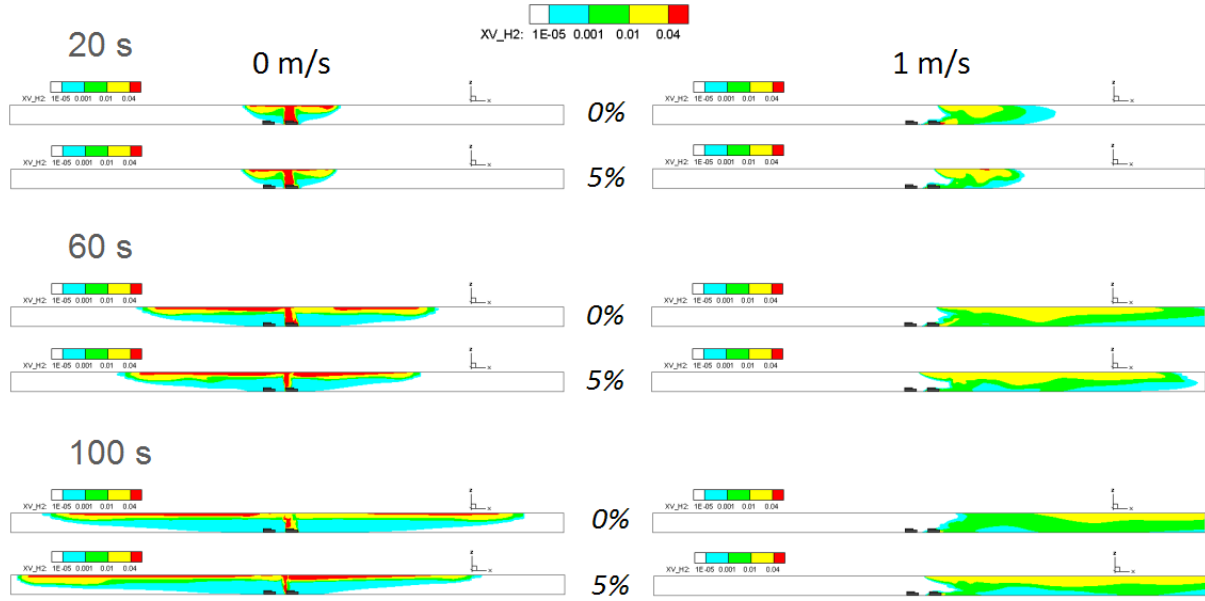


Figure 8. Mid-tunnel concentration contours at 20 s, 60 s and 100 s after the start of the release for the non-ventilated (left) and 1 m/s ventilation (right) cases. For each time, the zero slope (top) and 5% inclination (bottom) results are presented. The release duration is about 400 s (2 mm PRD)

After examining the general characteristics of the concentration field throughout the tunnel, we will now focus around the car, which is an area of high interest. At each subfigure of Figure 9, four contour slices are plotted. The one is at a XZ plane, just after the right side of the car, and the other three are at three YZ planes: 1) at the point of the PRD, 2) in front of the windscreen and 3) one meter in front of the car. Only the concentrations above the flammable are shown. At the same time the 4% vol. iso-surface is shown, with high translucency, in order to have an idea of the whole volume occupied from the flammable cloud. The color of the most dangerous concentration of 25%-35% vol. (due to high burning velocity) is stressed with an arrow at the first subfigure.

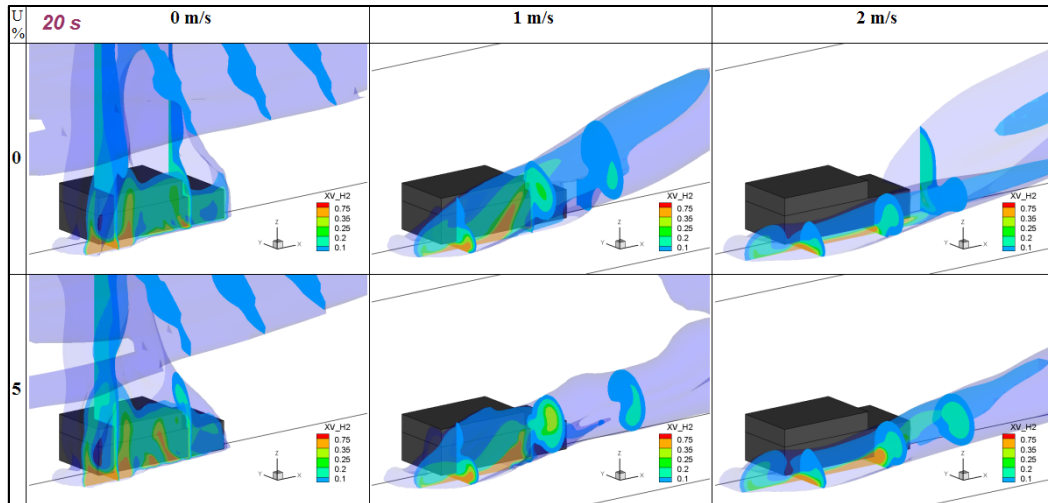


Figure 9. Above-flammable contour slices at 20 s after the start of the release. Cases of tunnels with 0% and 5% slope are presented, for three ventilation speeds each (0 m/s, 1 m/s and 2 m/s)

At the no-ventilation cases, the hydrogen, after impinging to the ground and spreading horizontally, surrounds the car. The buoyancy is the driving mechanism for the flow and as a result hydrogen rapidly reaches the ceiling of the tunnel above the car with high velocity and spreads again along the ceiling. The concentrations at the sides of the car are very high during the initial stages.



In case of ventilation, the hydrogen that comes out from the bottom of the car towards its sides interacts with the wind. This results in recirculating flow at the YZ planes at the sides of the car, which, along with the wind and the buoyancy, results in the inclined elongated vortices, one at each side of the car (Figure 9). The hydrogen spreads mainly through those vortices and it is transferred downwind. Counter-rotating vortices on top of the main vortices may also be formed and this, along with the effect of buoyancy, results in very complicated flow patterns. Depending on the wind strength, the cloud reaches the walls of the tunnel far downwind at an oblique angle and then spreads towards the ceiling of the tunnel and across the symmetry plane, having much lower concentrations there than in the no-ventilation cases. The flow and concentration fields are thus very different.

Concerning the most dangerous concentration range of 25%-35% v/v, we notice that in the no-ventilation cases, the relevant cloud stays in touch with the car sides, while in the ventilation cases it can be transferred alongside at distances up to one meter. This increases the possibilities of ignition from sources in the neighborhood of the car.

As the ventilation speeds gets higher, the elongated side-vortices get longer and more parallel to the ground. If we would look at similar contour slices as those of Figure 9 around the car at longer times, we would notice that the high-concentration clouds shrink. From that point of view, we could say that the most dangerous area is the area around the car for the first 20 s after the start of the release, regardless of the ventilation and of the inclination.

In order to see clearly the effect of inclination at ventilated tunnels, at Figure 10 (left) the evolution of flammable cloud for various slopes in the case of a ventilation speed of 1 m/s is presented. As expected, the maximum cloud volume increases as the inclination increases, but the differences are very small. Moreover, the 0% and 2.5% slope cases have almost the same evolution throughout the release. The 5% inclination case presents up to two times higher cloud volumes at times between 10 s and 40 s after the start of the release. If we compare Figure 10 with Figure 7, we can notice that the ventilation cases present about 4 times lower maximum flammable cloud volumes.

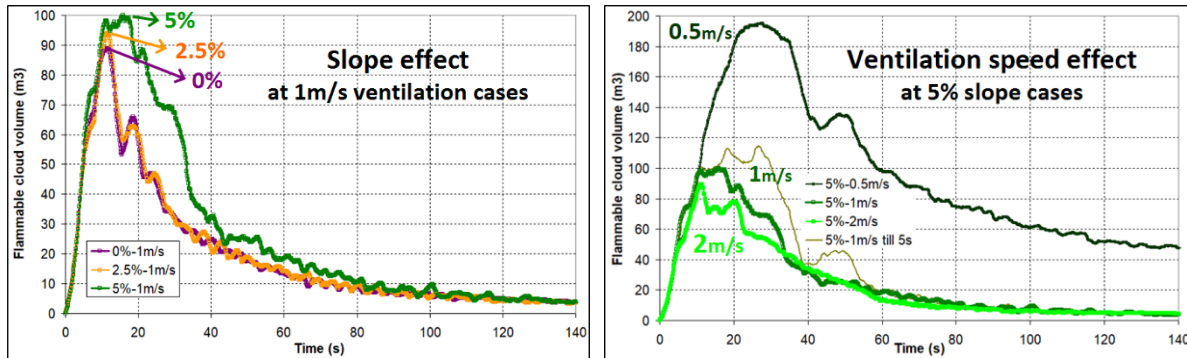


Figure 10. Whole-tunnel flammable cloud volume evolution for three inclinations with the same ventilation of 1 m/s (left) and for four different ventilation cases of a tunnel with a slope of 5% (right)

If we focus on the 5% slope tunnels (Figure 10, right) we notice that in general the higher the speed, the lower the maximum flammable cloud. If we ignore the too low ventilation case of 0.5 m/s, we see that the differences at cloud evolution are small. This is valid even in the case we stop the ventilation at 5 s after the start of the release. In conclusion, concerning the flammable cloud of the examined cases, the big difference is whether there is ventilation or not – the absolute value of ventilation (as long as it is above 0.5 m/s) and the possible inclination of the tunnel, are of secondary importance.

It should be noted that even if the maximums of the total nearly-stoichiometric hydrogen cloud volumes are comparable for all examined cases (not shown here), the distribution of the cloud around the car may be very different, especially between the ventilated and the no-ventilated cases. The inclination on the other hand has in general a minor role on the specific high-concentration cloud. The

results at the particular concentration range depend very much on the flow details below the car, which are difficult to predict.

Interestingly, it was observed that ventilation might also have negative effects for some spaces/ times. For instance, the case with no slope and 2 m/s ventilation, predicted two to three times bigger volumes with 25% - 35% concentration between 100 s and 250 s, than the other cases. This can be explained by the fact that at 2 m/s the dispersion is more intense and a significant nearly-stoichiometric region below the car is formed. If hydrogen is released from the bottom of the car, there might be cases where the concentrations can be close to the stoichiometric for relatively long periods of time. This raises a question about whether it is a good practice to have the PRD pointing towards the street.

Table 1, presents, as a summary of all cases, the maximum cloud in m<sup>3</sup> in the whole tunnel for various concentration ranges for all the ventilated and no-ventilated cases examined for all slopes. Inside the brackets, the time when the maximum cloud occurs, in seconds, is added. The values of Q9 equivalent volume [20] are also included. The 25% - 35% values and times are approximate.

Table 1. Summary of all cases examined – maximum cloud volumes and time they occur

Concent. range/ criterion	PRD 4mm				2mm			2mm		2mm				2mm	
	ventilation 0m/s				0m/s			0.5m/s		1m/s				1m/s till 5s	
	slope 0%	2.5%	5%	10%	0%	2.5%	5%	0%	5%	0%	2.5%	5%	5%	0%	5%
4%-75%	663 [41]	669 [42]	663 [42]	625 [41]	424 [76]	484 [77]	487 [82]	127 [12]	195 [28]	89.0[12]	93.9[12]	100 [16]	115 [27]	94.7[12]	89.4[11]
10%-75%	83.0[4.8]	83.1[5.2]	86.8[6.1]	90.1[6.0]	22.2[14]	22.8[15]	21.3[16]	17.1[3.9]	21.3[11]	18.4[7.4]	19.5[7.7]	23.4[8.1]	23.3[8.1]	24.4[8.7]	24.2[8.6]
25%-35%	8.61[2]	8.46[2]	8.47[2]	8.44[2]	1.61[2]	1.59[2]	1.59[2]	1.68[7]	1.71[7]	1.51[7]	1.65[7]	2.13[7]	2.17[7]	1.80[7]	2.23[7]
Q9	40.3[2.7]	40.5[2.7]	40.7[2.7]	41.4[2.8]	4.97[3.9]	4.95[17]	4.80[17]	5.06[3.9]	5.16[2.9]	5.22[6.8]	5.43[6.9]	6.32[7.1]	6.37[7.1]	6.04[7.3]	6.87[6.8]

We can see that the slope has a minor effect on the volume of maximum cloud and the time it happens: columns of the same color present in general similar values. If we compare the 4 mm and 2 mm PRD diameters, we see that the maximum flammable volume drops about 33%. From the other columns, we observe that the ventilation reduces the total flammable cloud by several times.

The most important concentration range concerning the safety though is the nearly-stoichiometric 25% - 35% vol. range. We observe that while there is a significant reduction by a factor of five when going from 4 mm PRD to 2 mm PRD, there is no systematic effect of either the inclination or the ventilation on the total nearly-stoichiometric cloud volumes.

If we want to have a first estimation of how hazardous a cloud is, without performing combustion simulations, we can use the Q9 criterion [20]. Q9 cloud ideally is a scaling of the non-homogeneous gas cloud to a smaller stoichiometric gas cloud that is expected to give similar explosion loads as the original cloud. We observe that while there is a reduction of Q9 by a factor of eight if 2 mm PRD is used instead of 4 mm PRD, there is generally no significant change due to the slope or the ventilation.

### 3.1 A note on the release direction

Since the downwards release direction appeared to present some disadvantages, two more release directions were roughly examined: upwards and backwards. The zero inclination and 0.5 m/s ventilation case was considered as reference case. It was found that the orientation of the release has significant effect. In both alternative release direction cases the maximum total nearly-stoichiometric cloud volume (25% - 35% v/v) was about 70 times smaller. The reason is that the nearly-stoichiometric cloud is confined at a small region around the core of the jet (see Figure 11), while at the downward case it spreads all around the car. Thus, alternative PRD release directions should be seriously considered when designing hydrogen cars.

Concerning the total flammable cloud, in upwards case it is slightly bigger compared to the downwards case (maximum of 142 m<sup>3</sup> instead of 126 m<sup>3</sup>) and it lasts much longer, having a maximum at 71 s instead of 13 s. In backwards release case, the maximum flammable cloud is about three times smaller compared to the downwards case.

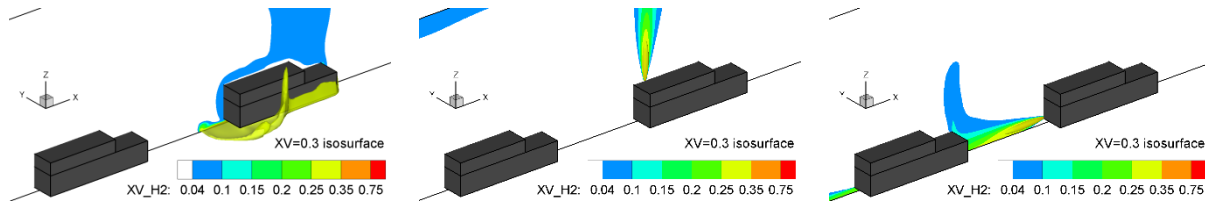


Figure 11. Mid-plane concentration contours and stoichiometric iso-surfaces at 10 s for downwards (left), upwards (middle) and backwards (right) release directions. The ventilation is 0.5 m/s in all cases

#### 4.0 CONCLUSIONS

In the current study the scenario of an accidental release of 6 kg of hydrogen from a car positioned in the middle of a 200 m long horseshoe-shaped tunnel was considered, in order to examine the effect of tunnel inclination on hydrogen dispersion, for various ventilation speeds.

It was observed that the area around the car is the most critical one, since, in all cases examined, regardless of the inclination and the ventilation considered, it is the only area that may present nearly-stoichiometric concentrations of hydrogen. The diameter/ position of PRD and the orientation of the release have a serious influence on safety. In general, the 2 mm PRD diameter can be considered safer than the 4 mm, since it presents about five times lower maximum of the nearly-stoichiometric cloud volumes. The default downwards hydrogen release direction below the car should be reconsidered, since it results in about 70 times higher maximum of the nearly-stoichiometric cloud volumes compared to the upwards or backwards directions at the examined cases.

The inclination, at both ventilated and non-ventilated tunnels, has small effect on the velocity and concentration field around the car during the initial stages of the release, especially concerning the more dangerous concentration ranges. It affects hydrogen dispersion at larger time and spatial scales where interesting phenomena may occur. The long-term influence of the inclination at non-ventilated tunnels is positive: the higher the inclination, the sooner hydrogen will reach nearly-zero concentrations. There are though cases/ places/ times where adverse effects may exist. For example, the total volume of flammable cloud inside the tunnel may be bigger in case of inclination. Special design recommendations for short inclined tunnels are currently not deemed necessary.

The ventilation has strong effect on the flow and concentration field of the tunnel and it usually overwhelms any stack effects due to inclination. In all ventilated cases of inclined and non-inclined tunnels examined, even with small wind, the total flammable cloud of the tunnel was several times smaller compared to the cases with no ventilation, regardless of the inclination. On the other hand, at the most flammable cloud volumes (25%-35% v/v), even if the cloud shape heavily depends on the wind speed, no systematic effect on the maximums of the total cloud volumes could be identified. It should be noted, that even if the ventilation has in general a positive effect in hydrogen safety, there may be cases with adverse effects. For example, the ventilation velocity increase does not always result in lower total cloud volumes. Another example is the 2 m/s ventilation case with no slope, which presented two to three times higher nearly-stoichiometric cloud volumes at mid-term of the release compared to all other cases examined. In short, even small ventilation is enough to severely reduce the flammable cloud volume, the ventilation does not seem to have a significant effect on the maximum of the total volume of the more dangerous nearly-stoichiometric concentrations and it may also cause adverse effects in some cases.

#### 5.0 ACKNOWLEDGMENTS

The research leading to these results was financially supported by the HyTunnel-CS which has received funding from the Fuel Cells and Hydrogen 2 Joint Undertaking under grant agreement No 826193. This Joint Undertaking receives support from the European Union's Horizon 2020 research and innovation programme, Hydrogen Europe and Hydrogen Europe research.

## REFERENCES

1. Venetsanos, A.G., Papanikolaou, E.A. and Bartzis, J.G., The ADREA-HF CFD code for consequence assessment of hydrogen applications, *International Journal of Hydrogen Energy*, **35**, No. 8, 2010, pp. 3908–3918.
2. Giannissi, S.G., Shentsov, V., Melideo, D., Cariteau, B., Baraldi, D., Venetsanos, A.G. and Molkov, V., CFD benchmark on hydrogen release and dispersion in confined, naturally ventilated space with one vent, *International Journal of Hydrogen Energy*, **40**, No. 5, 2015, pp. 2415–2429.
3. Zhao, S., Li, Y.Z., Kumm, M., Ingason, H. and Liu, F., Re-direction of smoke flow in inclined tunnel fires, *Tunnelling and Underground Space Technology*, **86**, 2019, pp. 113–127.
4. Tuovinen, H., Holmstedt, G. and Bengtson, S., Sensitivity Calculations of Tunnel Fires Using CFD, *Fire Technology*, **32**, No. 2, 1996, pp. 99–119.
5. Woodburn, P.J. and Britter, R.E., CFD Simulations of a Tunnel Fire - Part II, *Fire Safety Journal*, **26**, 1996, pp. 63–90.
6. Ji, J., Wan, H., Li, K., Han, J. and Sun, J., A numerical study on upstream maximum temperature in inclined urban road tunnel fires, *International Journal of Heat and Mass Transfer*, **88**, 2015, pp. 516–526.
7. Fan, C.G., Li, X.Y., Mu, Y., Guo, F.Y. and Ji, J., Smoke movement characteristics under stack effect in a mine laneway fire, *Applied Thermal Engineering*, **110**, 2017, pp. 70–79.
8. Musto, M. and Rotondo, G., Numerical comparison of performance between traditional and alternative jet fans in tiled tunnel in emergency ventilation, *Tunnelling and Underground Space Technology*, **42**, 2014, pp. 52–58.
9. Du, T., Yang, D. and Ding, Y., Driving force for preventing smoke backlayering in downhill tunnel fires using forced longitudinal ventilation, *Tunnelling and Underground Space Technology*, **79**, 2018, pp. 76–82.
10. Ballesteros-Tajadura, R., Santolaria-Morros, C. and Blanco-Marigorta, E., Influence of the slope in the ventilation semi-transversal system of an urban tunnel, *Tunnelling and Underground Space Technology*, **21**, No. 1, 2006, pp. 21–28.
11. Mukai, S., Suzuki, J., Mitsuishi, H., Oyakawa, K. and Watanabe, S., CFD simulation of diffusion of hydrogen leakage caused by fuel cell vehicle accident in tunnel, underground parking lot and multi-story parking garage, 19th Int. Technical Conf. on the Enhanced Safety of Vehicles (ESV), 6–9 June 2005, Washington D.C.
12. Seike, M., Kawabata, N., Hasegawa, M. and Tanaka, H., Heat release rate and thermal fume behavior estimation of fuel cell vehicles in tunnel fires, *International Journal of Hydrogen Energy*, **44**, No. 48, 2019, pp. 26597–26608.
13. Tolias, I.C., Giannissi, S.G., Venetsanos, A.G., Keenan, J., Shentsov, V., Makarov, D., Coldrick, S., Kotchourko, A., Ren, K., Jedicke, O., Melideo, D., Baraldi, D., Slater, S., Duclos, A., Verbecke, F. and Molkov, V., Best practice guidelines in numerical simulations and CFD benchmarking for hydrogen safety applications, *International Journal of Hydrogen Energy*, **44**, No. 17, 2019, pp. 9050–9062.
14. Birch, A.D., Brown, D.R., Dodson, M.G. and Swaffield, F., The structure and concentration decay of high pressure jets of natural gas, *Combustion Science and Technology*, **36**, Nos. 5–6, 1984, pp. 249–261.
15. Tolias, I.C. and Venetsanos, A.G., Comparison of convective schemes in Hydrogen Impinging Jet CFD simulation, 6th International Conference on Hydrogen Safety, 19–21 October, 2015, Yokohama, Japan.
16. Wang, F., Wang, M., He, S. and Deng, Y., Computational study of effects of traffic force on the ventilation in highway curved tunnels, *Tunnelling and Underground Space Technology*, **26**, 2011, pp. 481–489.
17. Ismail, I., Tsukikawa, H. and Kanayama, H., Modelling Considerations in the Simulation of Hydrogen Dispersion within Tunnel Structures, *Journal of Applied Mathematics*, 846517, 2012, 13 pp.
18. Amouzandeh, A., Zeiml, M. and Lackner, R., Real-scale CFD simulations of fire in single- and double-track railway tunnels of arched and rectangular shape under different ventilation conditions, *Engineering Structures*, **77**, 2014, pp. 193–206.
19. Haghighat, A. and Luxbacher, K., Determination of critical parameters in the analysis of road tunnel fires, *International Journal of Mining Science and Technology*, **29**, 2019, pp. 187–198.
20. Middha, P., Hansen, O.R., CFD simulation study to investigate the risk from hydrogen vehicles in tunnels, *International Journal of Hydrogen Energy*, **34**, 2009, pp. 5875–5886.